Supporting Information

Exploring the promotional effects of K, Sr and Mg on the catalytic stability of red mud for the synthesis of glycerol carbonate from renewable glycerol

Bikashbindu Das, Kaustubha Mohanty*

Department of Chemical Engineering, Indian Institute of Technology Guwahati, Guwahati 781039, India.

*Corresponding author Email: kmohanty@iitg.ac.in; Tel: +91-361-2582267

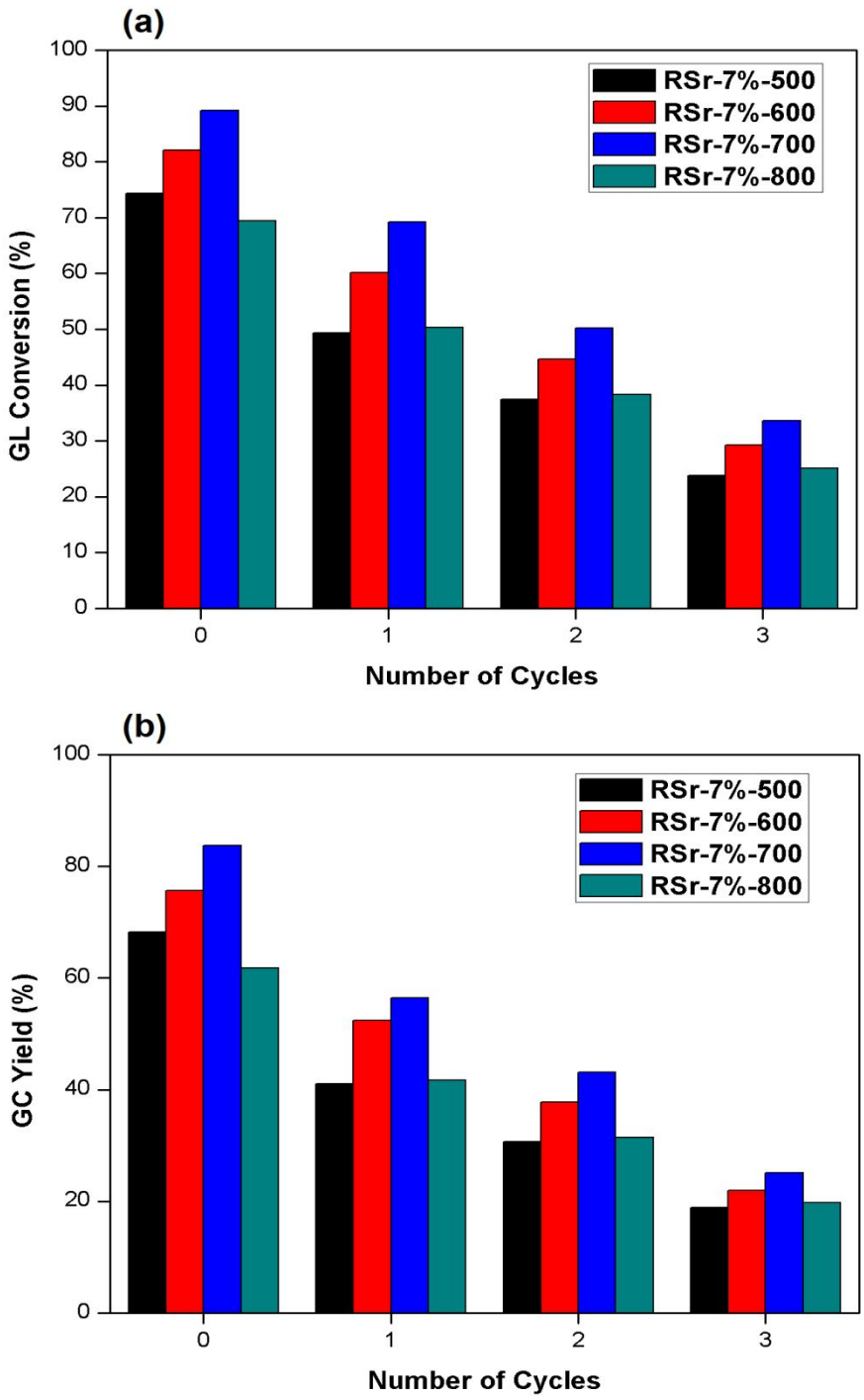

Figure S1. Effect of calcination temperatures on the catalytic activity and stability of RSr-7% catalyst. (a) effect on GL conversion, (b) effect on GC yield. Reaction conditions: GL/DMC molar ratio = 1:3, time = 90 min, T = 75 ^{o}C, catalyst loading = 10 wt.%.

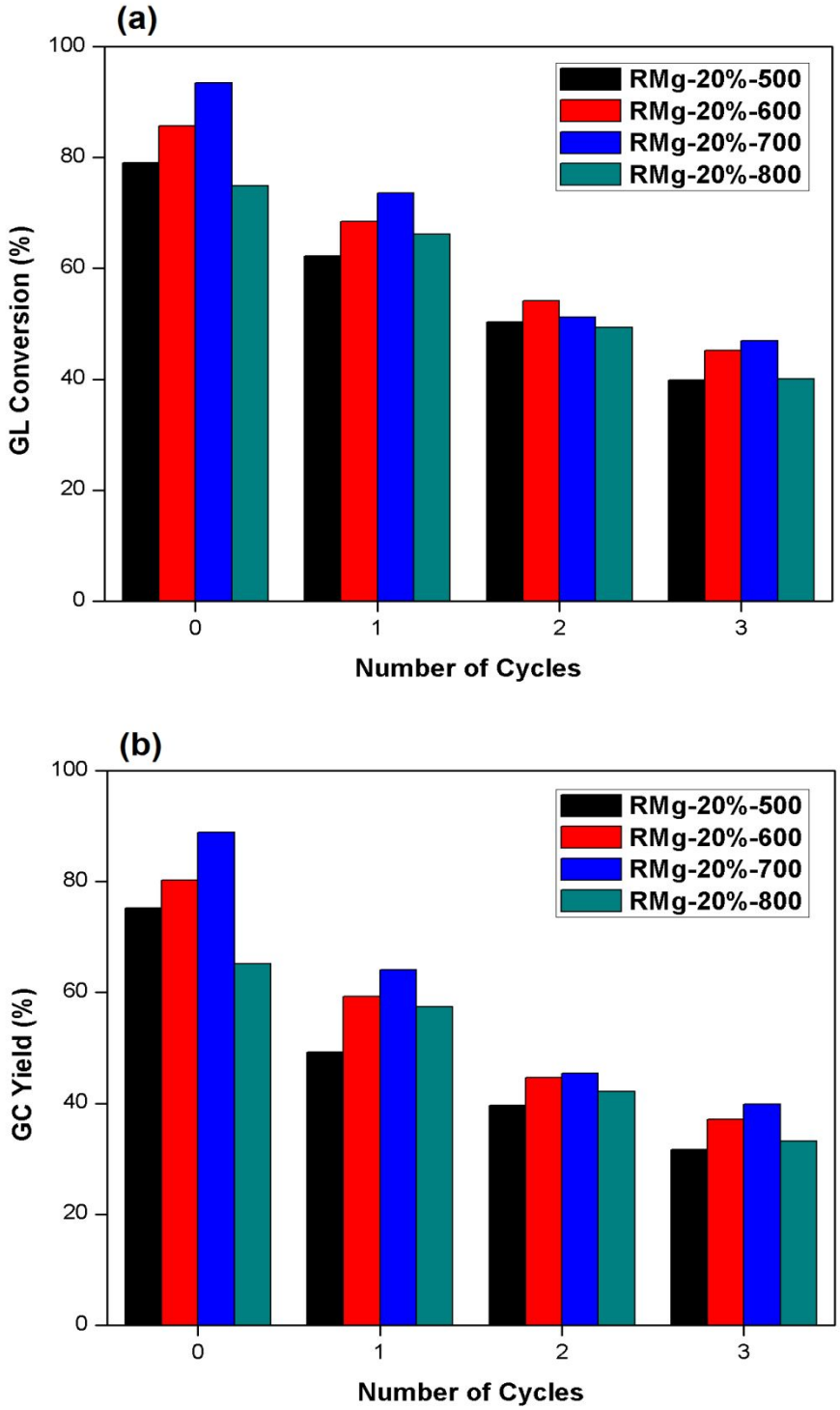

Figure S2. Effect of calcination temperatures on the catalytic activity and stability of RMg-20% catalyst. (a) effect on GL conversion, (b) effect on GC yield. Reaction conditions: GL/DMC molar ratio = 1:3, time = 90 min, T = 75 ^{o}C, catalyst loading = 10 wt.%

Thermal gravimetric analysis (TGA)

From the TGA profile, the mass loss occurred up to a temperature of 160 ^{o}C could be due to the removal of physically bound water from the catalyst surface. At higher temperature range between 200 ^{o}C to 460 ^{o}C the mass loss observed was due to the removal of chemically bound water molecules. Further increase in temperature from 500 ^{o}C to 875 ^{o}C produced another mass loss region, which could be assign to the decomposition of nitrate, and carbonate groups of the catalyst.

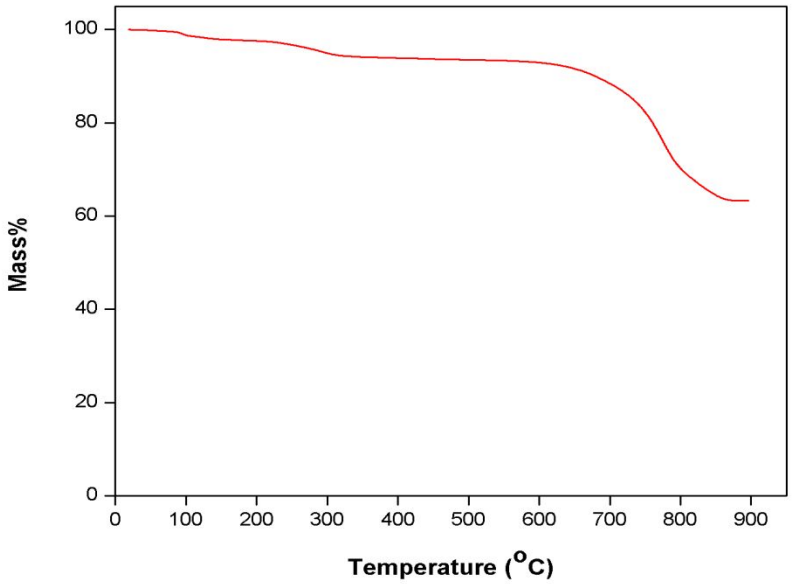

Figure S3. TGA profile of RK-30% catalyst

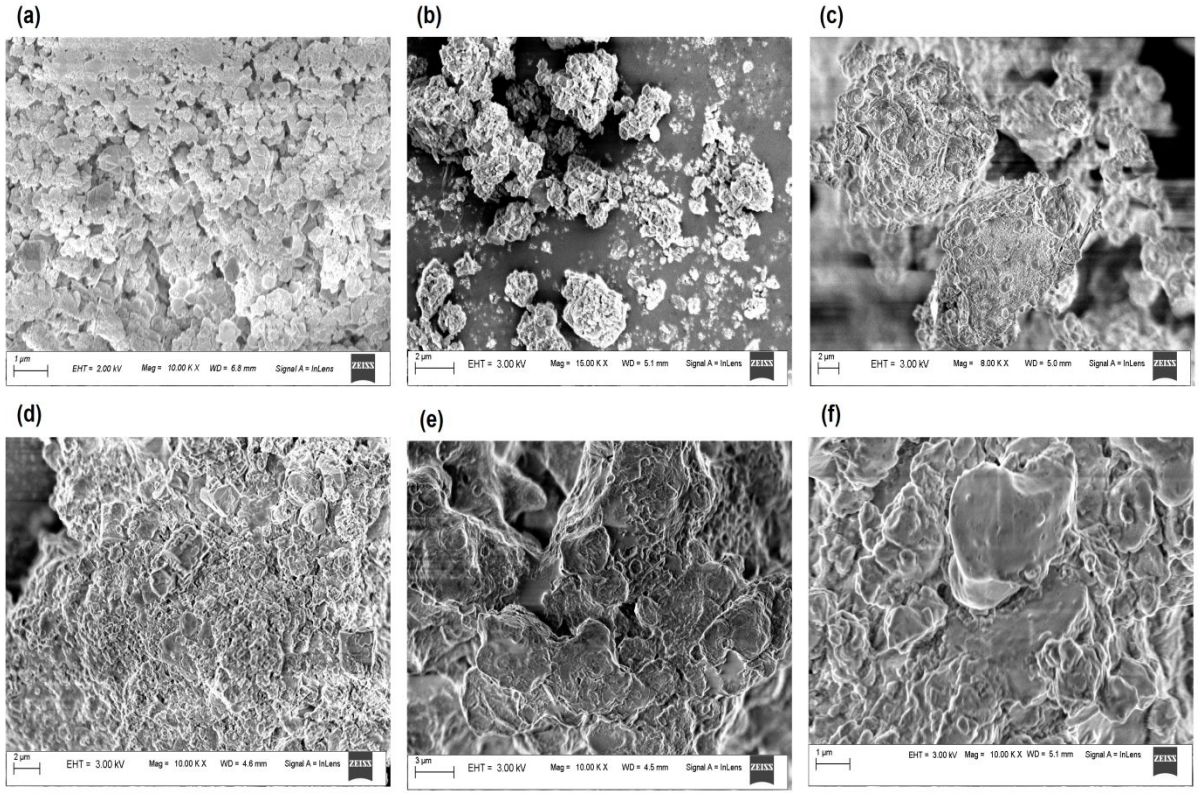

Figure S4. Surface morphology of (a) RM, (b) RK-30%-100, (c) RK-30%-500, (d) RK-30%-600, (e) RK-30%700, (f) RK-30%-800.

Table S1. FESEM-EDX analysis of fresh and the fifth reuse RK-30%-800 catalyst

Elements	C	O	Fe	Al	Si	Ti	Na	Ca	K
RK-30%-800	10.4	39.9	15.8	4.9	2.0	3.1	3.6	0.2	20.1
Fifth reuse of RK-30%-800	13.0	46.5	14.1	4.9	6.2	2.3	2.1	0.2	10.7

Table S2. Surface area and pore size analysis of different catalysts

Catalyst	Surface area (m^2 g^{-1})	Average pore size (nm)	Total pore volume (cm^3 g^{-1})

RM	11.66	19.26	0.0561
RK-30%-100	4.40	26.11	0.028
RK-30%-500	5.0	11.39	0.0142
RK-30%-600	6.54	13.27	0.021
RK-30%-700	1.32	29.53	0.0097
RK-30%-800	1.36	18.54	0.0063

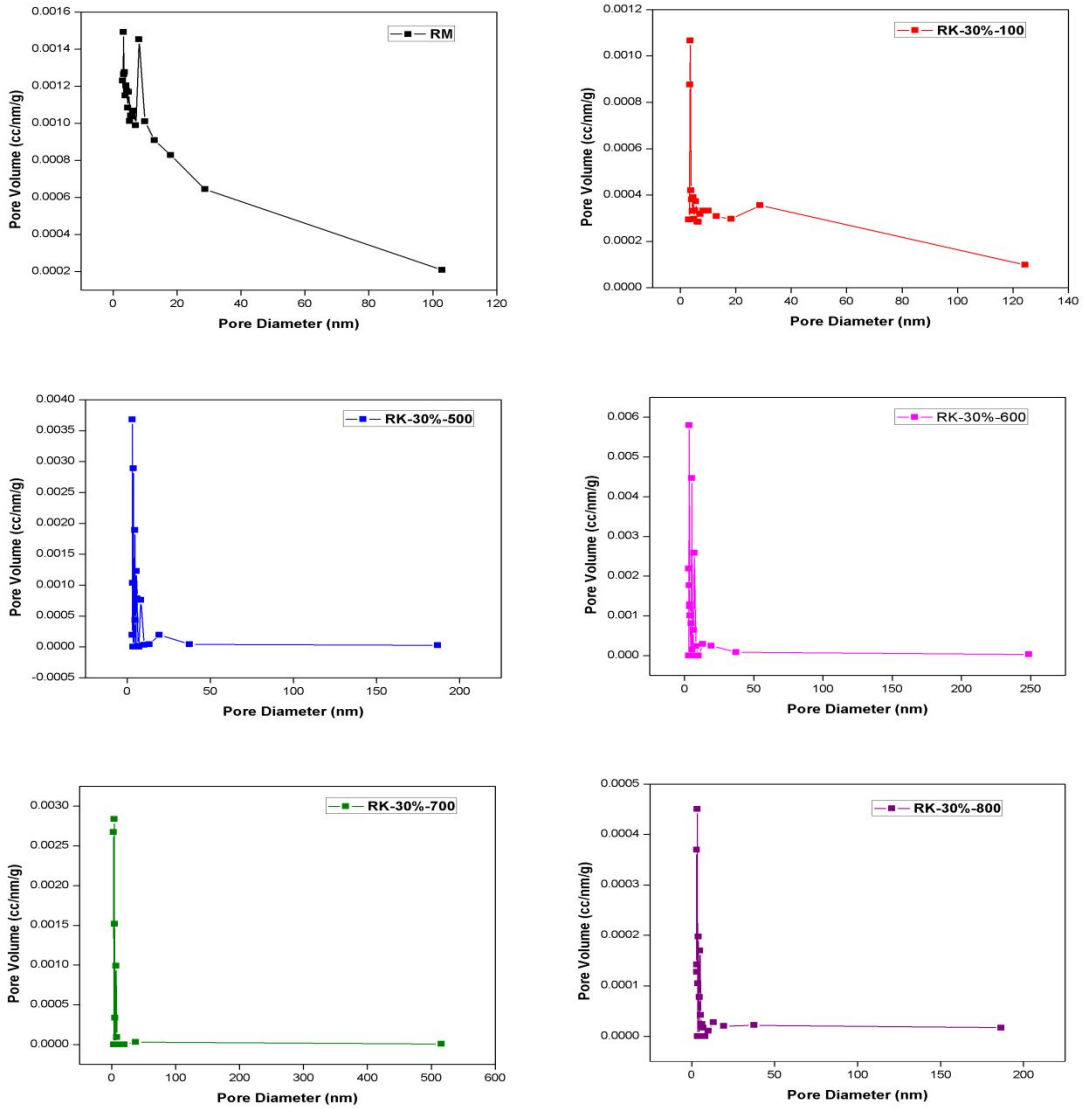

Figure S5. Pore size distribution curve of different RM based catalysts.

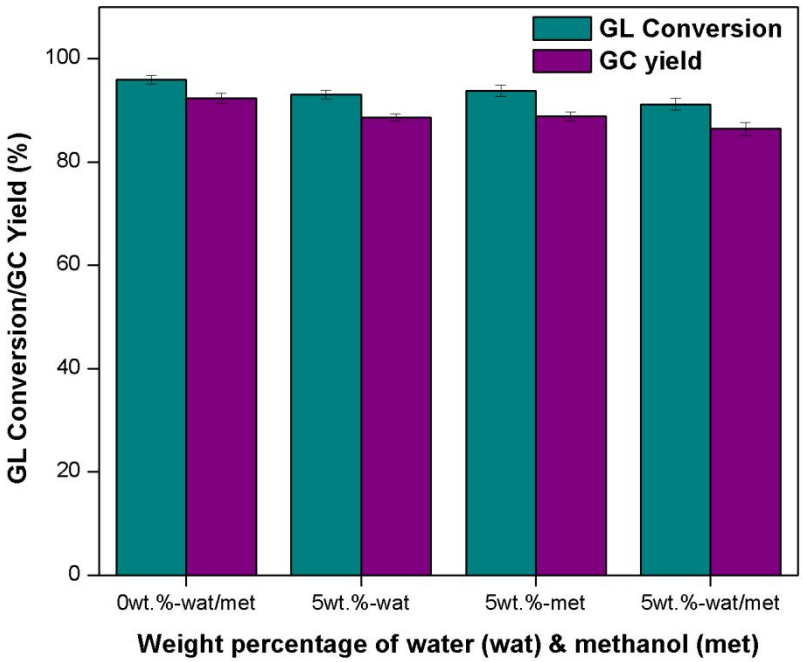

Figure S6. Activity of the RK-30%-800 catalyst in the presence of water (wat) and methanol (met) as impurities. Reaction conditions: GL/DMC molar ratio = 1:3, time = 90 min, T = 75°C and catalyst loading = 10 wt.%.

Langmuir-Hinshelwood model for kinetic analysis

The variation of reaction rate beyond a stirring speed of 600 rpm was observed to be insignificant, which confirmed the absence of external mass transfer limitations. The approximate particle size of the catalyst taken for the reaction was less than 15 μm for which the Weisz-Prater parameter remains less than 1, thus, the internal mass transfer limitations could be neglected.[1,2]

Following are the necessary assumption considered for the development of the kinetic model

i) The rate was surface reaction controlling and all other steps except the surface reaction were considered to be in equilibrium.

ii) Although, the existence of reversible reaction between GC and methanol was observed at longer reaction period (after 90 min), however, the rate of reverse reaction was not significant and therefore, was neglected for developing the kinetic model.

iii) The Concentration of DMC throughout the reaction was considered as same, since, it was taken in excess.

Different reaction steps for production of GC by the transesterification of GL with DMC are provided below.

GL adsorption on the surface of the catalyst:

$$GL + S \leftrightarrow GL.S \tag{S1}$$

DMC adsorption on the surface of the catalyst:

$$DMC + S \leftrightarrow DMC.S \tag{S2}$$

Reaction between the adsorbed GL and DMC on the surface of the catalyst:

$$GL.S + DMC.S \leftrightarrow GC.S + MET.S \tag{S3}$$

Desorption of GC and methanol from the surface of the catalyst:

$$GC.S \leftrightarrow GC + S \tag{S4}$$

$$MET.S \leftrightarrow MET + S \tag{S5}$$

By considering the assumption (ii), the rate of the reaction can be expressed as:

$$-r = -\frac{dC_{GL}}{dt} = k_S C_{GL.S} \,.\, C_{DMC.S} - k'_S C_{GC.S} \,.\, C_{MET.S} \tag{S6}$$

Or, $$-\frac{dC_{GL}}{dt} = k_S(C_{GL.S} \,.\, C_{DMC.S} - \frac{1}{K_S} C_{GC.S} \,.\, C_{MET.S}) \tag{S7}$$

where, K_S can be defined as, $K_S = \frac{k_S}{k_S'}$

The concentration of different adsorbed species are as expressed below.

$$C_{GL.S} = K_{GL} C_{GL} C_v \quad \text{(S8)}$$

$$C_{DMC.S} = K_{DMC} C_{DMC} C_v \quad \text{(S9)}$$

$$C_{GC.S} = K_{GC} C_{GC.} C_v \quad \text{(S10)}$$

$$C_{MET.S} = K_{MET} C_{MET.} C_v \quad \text{(S11)}$$

C_v is the concentration of vacant site on the catalyst.

By putting the value of Eq. S8 to S11 on Eq. S7, the rate expression becomes:

$$-\frac{dC_{GL}}{dt} = k_S \,.\, K_{GL} \,.\, K_{DMC} \left(C_{GL} \,.\, C_{DMC} - \frac{K_{GC} \,.\, K_{MET}}{K_S \,.\, K_{GL} \,.\, K_{DMC}} C_{GC} \,.\, C_{MET} \right) {C_v}^2 \quad \text{(S12)}$$

Vacant site concentration C_v can be presented as:

$$C_v = \frac{C_o}{1 + C_{GL.S} + C_{DMC.S} + C_{GC.S} + C_{MET.S}} \quad \text{(S13)}$$

where, C_o is the total concentration of active sites on the catalyst.

Eq. S12, after putting the value of Eq. S13 becomes,

$$-\frac{dC_{GL}}{dt} = \frac{k_S \,.\, K_{GL} \,.\, K_{DMC} \left(C_{GL} \,.\, C_{DMC} - \frac{K_{GC} \cdot K_{MET}}{K_S \cdot K_{GL} \cdot K_{DMC}} C_{GC} \,.\, C_{MET} \right) {C_o}^2}{(1 + C_{GL.S} + C_{DMC.S} + C_{GC.S} + C_{MET.S})^2} \quad \text{(S14)}$$

By neglecting the reverse reaction as per the assumption (iii) and considering the DMC concentration constant as per the assumption (iv), the rate expression reduced to,

$$-\frac{dC_{GL}}{dt} = (KwC_{GL}) \quad \text{(S15)}$$

where, $Kw = k_S K_{GL} K_{DMC} {C_o}^2$; w is the weight of the catalyst.

The final rate expression in terms of conversion after integration of Eq. (S15) can be expressed as:

$$-\ln\left(1 - X_{GL}\right) = Kwt \tag{S16}$$

The plot of $-\ln\left(1 - X_{GL}\right)$ vs t at different reaction temperatures are shown in Fig. S7.

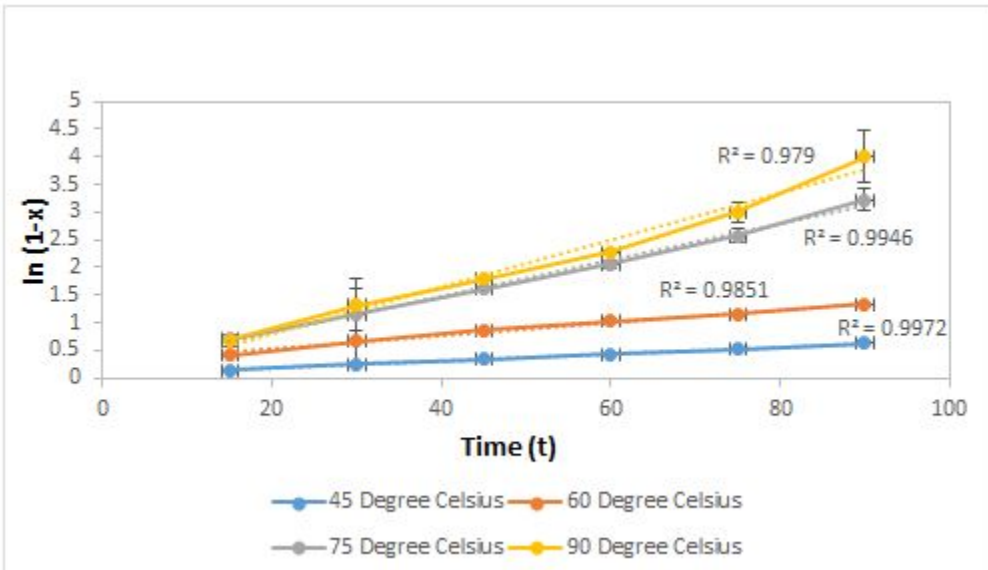

Figure S7. Kinetic plot of the transesterifcation of GL by using RK-30%-800 catalyst

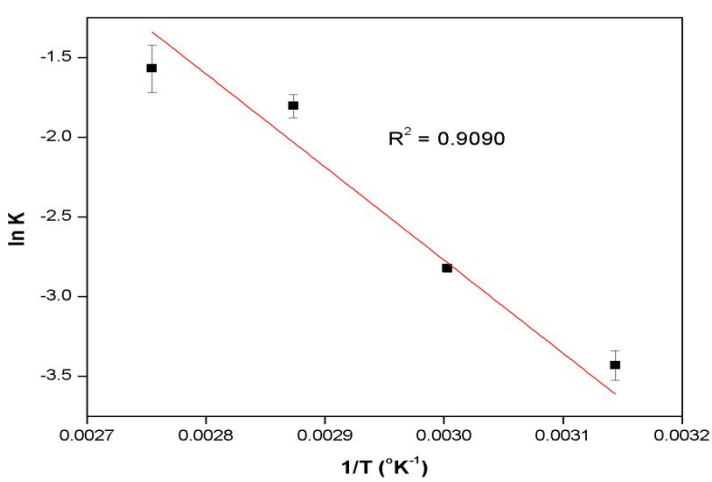

Figure S8. Arrhenius plot for kinetic energy calculation

References

(1) Singh, D.; Reddy, B.; Ganesh, A.; Mahajani, S. Zinc/lanthanum Mixed-Oxide Catalyst for the Synthesis of Glycerol Carbonate by Transesterification of Glycerol. *Ind. Eng. Chem. Res.* **2014**, *53* (49), 18786–18795.

(2) Zhu, J.; Li, M.; Lu, M.; Zhu, J. Effect of Structural Properties on Catalytic Performance in Citral Selective Hydrogenation over Carbon-Titania Composite Supported Pd Catalyst. *Catal. Sci. Technol.* **2013**, *3* (3), 737–744.